Research Square

Preprints are preliminary reports that have not undergone peer review.
They should not be considered conclusive, used to inform clinical practice,
or referenced by the media as validated information.

Panel-Gene Transcriptomic Associations in Amyotrophic Lateral Sclerosis: a donor-resolved seven-cohort analysis of a locked 468-gene detoxification panel

Mark E. McCaulley

mark@siriusneuroscience.com

Sirius Neuroscience, LLC https://orcid.org/0000-0003-2059-622X

Research Article

Keywords: amyotrophic lateral sclerosis, motor neuron, spinal cord, transcriptomic meta-analysis, aquaporin, APOE, iron, oxidative stress

Posted Date: October 30th, 2026

DOI: https://doi.org/10.21203/rs.3.rs-11552529/v1

License: This work is licensed under a Creative Commons Attribution 4.0 International License.
Read Full License

Additional Declarations: The authors declare potential competing interests as follows: The author is the sole inventor on a filed patent application relating to panel-based research scoring methods that use the locked 468-gene list reported here. The application did not determine gene membership, the high-confidence rule or the reported results. Academic reuse of the deposited panel and code does not require a license from the author. The author declares no other competing interests.

Abstract

Amyotrophic lateral sclerosis (ALS) was analysed in seven adult central-nervous-system cohorts (GSE153960, GSE26927, GSE76220, GSE19332, GSE68605, GSE56500 and GSE18920; 220 ALS and 97 control donors) with a locked 468-gene redox, metal, xenobiotic and barrier panel. Each cohort entered as one estimate per donor: bulk spinal cord in GSE153960, with cervical, lumbar and thoracic counts summed per donor and sequencing platform modelled; donor averages in GSE26927; motor-neuron samples only in GSE18920; and gene-level summaries for the two exon-array cohorts. Random-effects meta-analysis yielded 449 analysable genes, 33 at false-discovery rate (FDR) < 0.05 and 28 high-confidence genes (FDR < 0.05, measured in ≥ 3 cohorts, direction-concordant in ≥ 70% of cohorts, nominally significant in ≥ 2 cohorts); 25 of the 28 were higher in ALS, and the median I^2 among them was 56.7%. Eight genes — ABCA1, APOE, AQP1, AQP4, SLC30A7, SLC40A1, SLC7A11 and SP1 — remained high-confidence in every sensitivity analysis of the primary design, including adjustment for neuronal, myeloid and astrocytic marker scores, which reduced the high-confidence set to 11–14 genes; six of the eight did so when the largest cohort, GSE153960, was left out. Against coverage-matched random gene sets, the panel was not over-represented among FDR-significant (35 v 41.5 expected) or high-confidence genes (29 v 26), and the Hartung–Knapp–Sidik–Jonkman adjustment left one gene. These results revise an earlier locked analysis of the same seven cohorts (456 analysable, 26 FDR-significant and 22 high-confidence genes; median I^2 60.6%) whose inputs pooled all tissues of GSE153960 and both tissue compartments of GSE18920 and counted GSE26927 replicate arrays as separate subjects. Every number is transcript abundance in postmortem tissue.

Companion note

This is the disease-restricted amyotrophic lateral sclerosis (ALS) analysis of the locked 468-gene panel and high-confidence rule defined in the companion methods-and-panel manuscript (1). It is not a pooled cross-disease analysis. Parallel companion manuscripts apply the same panel and rule to Alzheimer disease (2), Parkinson disease (3), multiple sclerosis (4) and autism spectrum disorder (5). Panel construction is described there and is not repeated here; the ALS datasets, contrasts and statistics are given below.

One-sentence summary

Across seven adult ALS cohorts analysed at the donor level, 28 panel genes meet a locked high-confidence rule and 8 of them hold under every sensitivity analysis of the primary design (6 of the 8 when the largest cohort is left out), but the panel as a whole changes no more often than comparable genes elsewhere in the transcriptome.

What this analysis reports

Three findings carry the paper. First, a set of panel transcripts is consistently shifted in ALS across these seven cohorts: 28 genes meet the locked high-confidence rule, and 8 of them (ABCA1, APOE, AQP1, AQP4, SLC30A7, SLC40A1, SLC7A11, SP1) survive every sensitivity analysis of the primary design, including adjustment for cell composition (six of the eight without GSE153960). They span cholesterol efflux, water channels, iron export, zinc transport and the cystine–glutamate antiporter. Second, most of the remaining signal travels with the glial and myeloid response of ALS tissue: adjusting the two bulk cohorts for myeloid marker expression halves the high-confidence set. Third, the panel as a whole is not special. Detoxification-panel genes change in ALS at about the rate of comparable genes elsewhere in the genome, and a permissive, consistency-based layer adds at most about a dozen genes beyond chance. The paper therefore reports three tiers of evidence — a robust core, the primary result and an exploratory layer — and a coverage-matched background test that measures how much each tier adds.

Introduction

Amyotrophic lateral sclerosis (ALS) is a progressive and fatal neurodegenerative disease caused by degeneration of upper and lower motor neurons (6,7). It has a lifetime risk of about 1 in 400 and a median survival of two to five years from symptom onset (8). Pathogenic variants in SOD1, TARDBP, FUS, C9orf72 and more than 40 further loci have been identified (9,10), yet the basis of selective motor-neuron vulnerability remains incompletely understood.

SOD1, the first ALS gene identified (11), encodes Cu/Zn superoxide dismutase, placing a detoxification-pathway enzyme among established ALS genes. That genetic fact is not a demonstration that panel transcripts measure impaired detoxification. Oxidative stress, mitochondrial failure and protein aggregation (12) and disruption of the blood–spinal-cord barrier (13–15) have all been implicated. These processes have not, to my knowledge, been examined together on one pre-specified gene set across several independent human ALS cohorts analysed at the level of the donor.

This paper applies the locked 468-gene panel (1, 16) to seven ALS cohorts. The panel comprises CORE redox/metal/xenobiotic/barrier genes (n = 394), CORE cGAS–STING (n = 12), CORE ferroptosis/iron/NRF2 (n = 10), a 40-gene SENSITIVITY layer and a 12-gene placental/sex-steroid module (labelled "ASD-maternal module" in the frozen panel file). The paper also revises an earlier locked analysis of the same cohorts. A re-audit found that three of the earlier inputs did not measure what the earlier text described, and the corrected analysis is reported here alongside the earlier result.

Results

Cohorts and units of analysis

Seven human cohorts entered the meta-analysis (Table 1). Two are bulk spinal cord (GSE153960, GSE26927); five are laser-capture-microdissected (LCM) motor neurons (GSE76220, GSE19332,

GSE68605, GSE56500, GSE18920). Each cohort contributed one estimate per gene, computed on one value per donor.

Four features of the source data governed that choice. GSE153960 lists 1,838 samples from 478 donors across 12 tissue labels and two sequencing platforms; its 1,300 "ALS Spectrum MND" and "Non-Neurological Control" samples come from 337 donors, about 3.9 samples per donor, and only 452 of them (35%) are spinal cord. The primary GSE153960 estimate therefore used spinal cord only, summing cervical, lumbar and thoracic counts within each donor (169 ALS, 57 control donors) and modelling platform. GSE18920 contains the same 22 donors twice, once as LCM motor-neuron-enriched samples and once as anterior horn; only the motor-neuron samples were used. GSE26927 contains 10 ALS and 10 control cervical-cord samples from 9 and 7 donors; replicate arrays were averaged within donor. GSE76220 lists 21 samples, but one control (GSM1977027) is absent from the NCBI-generated counts, leaving 13 ALS and 7 controls.

The two exon-array cohorts (GSE56500, GSE18920; Affymetrix GPL5188) carry a median of 10 core probesets per gene. Selecting the probeset with the smallest P value, the rule used for other arrays, makes 58% of genes nominally significant in these cohorts against 12–14% of individual probesets. The selected estimates are therefore biased toward extreme values. Probesets were averaged within each transcript cluster before testing, which brings the proportion of nominally significant genes to about 20%. On GPL570 (about two probes per gene) the smallest-P rule was retained, as in the locked pipeline; mean-probe collapse is reported as a sensitivity analysis.

Table 1
Cohorts, units of analysis and inputs to the primary meta-analysis.

Cohort	Platform	Tissue	ALS / control (units)	Primary input	Reproduction from source
GSE153960 (17,18)	RNA-seq (GPL16791, GPL24676)	Bulk spinal cord	169 / 57 donors (452 samples)	Counts summed per donor across cord levels; PyDESeq2, ~platform + group	NCBI counts, SHA-256 verified
GSE26927 (19)	Illumina HumanRef-8 (GPL6255)	Bulk cervical cord	9 / 7 donors (10 / 10 arrays)	Replicate arrays averaged per donor; limma	GEO2R table reproduced exactly
GSE76220 (20)	RNA-seq (GPL9115)	LCM lumbar motor neurons	13 / 7	DESeq2 on NCBI counts	$\log_2$FC r = 0.9998 v GEO2R
GSE19332 (21)	Affymetrix U133 Plus 2.0 (GPL570)	LCM cervical motor neurons (CHMP2B)	3 / 7	limma; smallest-P probe	GEO2R table reproduced exactly
GSE68605 (22)	Affymetrix U133 Plus 2.0 (GPL570)	LCM motor neurons (C9ORF72)	8 / 3	limma; smallest-P probe	GEO2R table reproduced exactly
GSE56500 (23)	Affymetrix exon (GPL5188)	LCM lower motor neurons	6 (3 sporadic, 3 C9ORF72) / 6	limma on transcript-cluster means	GEO2R table reproduced exactly
GSE18920 (24)	Affymetrix exon (GPL5188)	LCM motor-neuron-enriched (anterior-horn samples excluded)	12 / 10	limma on transcript-cluster means	GEO2R table reproduced exactly

All contrasts are ALS minus control. Units are donors except where noted; one sample per donor unless stated. "Reproduction from source" refers to the per-cohort table regenerated from the GEO series matrix or NCBI-generated counts. LCM = laser-capture microdissection.

Primary result: seven-cohort random-effects meta-analysis

Of the 468 panel genes, 449 were measured in at least two cohorts (240 in all seven). Thirty-three reached Benjamini–Hochberg FDR < 0.05 across the analysable panel genes (25), and 28 met the locked high-confidence rule (Table 2, Fig. 1; per-cohort direction and significance in Table S3). Twenty-five of the 28 were higher in ALS; PINK1, HMOX2 and CYP51A1 were lower. The median I^2 among high-confidence

genes was 56.7%, so pooled effects should be read as directionally reproducible under substantial between-cohort heterogeneity, not as homogeneous effects. The five FDR-significant genes that failed the rule (CHST5, SLC11A2, HPGDS, HSD17B1, SLC22A5) were each nominally significant in only one cohort (Table S7).

The high-confidence genes fall into four groups by function. Water channels and lipid efflux: AQP1 (+ 1.36), AQP4 (+ 1.27), APOE (+ 1.30) and ABCA1 (+ 0.88). Iron and ferroxidase: SLC40A1 (+ 0.75), CP (+ 1.00) and FTL (+ 0.66). Metal transport: SLC30A7 (+ 0.32), SLC39A1 (+ 0.27) and SLC39A14 (+ 0.50). NRF2-associated and redox transcripts: SLC7A11 (+ 0.86), NQO1 (+ 0.52), HMOX1 (+ 0.34), SOD2 (+ 0.54) and BACH1 (+ 0.23). A group of xenobiotic and sterol enzymes (CYP1B1, CYP4F11, CYP7B1, CYP51A1, GSTCD, ABCC4) and IFI16, SIRT1, LRP1, ATP1B2, SP1, PINK1 and HMOX2 complete the set. These groupings describe gene function; they are not measured pathway activity.

Table 2
The 28 high-confidence panel genes of the seven-cohort ALS random-effects meta-analysis, ordered by FDR.

Gene	k	Pooled log_2FC	95% CI	I^2 (%)	BH-FDR	Subgroup signal	Robust core
SLC30A7	7	+ 0.32	+ 0.23 to + 0.41	3	1.2×10^{-9}	both	yes
ABCA1	7	+ 0.88	+ 0.60 to + 1.16	50	1.4×10^{-7}	both	yes
ABCC4	7	+ 0.29	+ 0.20 to + 0.38	0	1.4×10^{-7}	both	
AQP1	7	+ 1.36	+ 0.86 to + 1.86	77	8.9×10^{-6}	both	yes
APOE	7	+ 1.30	+ 0.80 to + 1.80	84	2.8×10^{-5}	both	yes
PINK1	7	-0.21	-0.30 to -0.13	0	7.1×10^{-5}	both	
CYP4F11	5	+ 0.43	+ 0.25 to + 0.62	0	2.0×10^{-4}	both	
AQP4	7	+ 1.27	+ 0.72 to + 1.83	75	3.1×10^{-4}	LCM	yes
HMOX1	6	+ 0.34	+ 0.19 to + 0.48	4	3.6×10^{-4}	both	
SLC7A11	6	+ 0.86	+ 0.46 to + 1.25	60	7.1×10^{-4}	both	yes
SOD2	7	+ 0.54	+ 0.29 to + 0.80	43	1.3×10^{-3}	both	
SLC39A1	7	+ 0.27	+ 0.14 to + 0.41	22	2.9×10^{-3}	both	
SP1	7	+ 0.53	+ 0.26 to + 0.79	78	2.9×10^{-3}	both	yes
IFI16	7	+ 0.97	+ 0.48 to + 1.46	79	2.9×10^{-3}	both	

Gene	k	Pooled log_2FC	95% CI	I^2 (%)	BH-FDR	Subgroup signal	Robust core
SLC39A14	7	+ 0.50	+ 0.25 to + 0.76	36	3.5×10^{-3}	LCM	
HMOX2	7	-0.29	-0.44 to -0.14	16	4.4×10^{-3}	both	
SLC40A1	7	+ 0.75	+ 0.34 to + 1.16	84	8.7×10^{-3}	LCM	yes
SIRT1	7	+ 0.28	+ 0.12 to + 0.43	39	9.3×10^{-3}	LCM	
BACH1	7	+ 0.23	+ 0.10 to + 0.36	21	9.3×10^{-3}	bulk	
ATP1B2	7	+ 0.75	+ 0.33 to + 1.17	75	9.3×10^{-3}	LCM	
GSTCD	7	+ 0.36	+ 0.16 to + 0.57	67	9.3×10^{-3}	both	
CP	7	+ 1.00	+ 0.41 to + 1.58	82	1.5×10^{-2}	both	
LRP1	7	+ 0.40	+ 0.16 to + 0.64	56	1.8×10^{-2}	LCM	
FTL	7	+ 0.66	+ 0.24 to + 1.08	84	3.0×10^{-2}	both	
CYP7B1	7	+ 0.38	+ 0.14 to + 0.63	57	3.1×10^{-2}	LCM	
CYP1B1	7	+ 0.73	+ 0.25 to + 1.20	71	3.7×10^{-2}	bulk	
NQO1	7	+ 0.52	+ 0.18 to + 0.85	78	3.7×10^{-2}	LCM	
CYP51A1	5	-0.38	-0.63 to -0.12	55	4.8×10^{-2}	LCM	

Pooled log_2 fold-change (ALS v control) from inverse-variance DerSimonian–Laird random-effects meta-analysis (26). k = contributing cohorts. BH-FDR across the 449 analysable panel genes. Subgroup signal

= compartment in which a separate random-effects pool reached P < 0.05 (LCM motor-neuron cohorts, k ≤ 5; bulk-cord cohorts, k ≤ 2); this subgroup split was defined after the results were seen and is descriptive (Table S4). Robust core = high-confidence in every analysis in Fig. 2.

The robust core and the sensitivity analyses

Eight further analyses each varied one choice (Table 3, Fig. 2). Restricting GSE153960 to cervical or lumbar cord, averaging all array probes, or reverting the exon arrays to the smallest-P probeset changed the high-confidence count to between 27 and 37 genes. Removing the ten genes added to the panel at the freeze (CUL3, RBX1, AIFM2, GCH1, TF, TFRC, GLO1, HAGH, MFSD2A, FXN) changed nothing: none of the ten was FDR-significant. Eight genes were high-confidence in every one of these analyses: ABCA1, APOE, AQP1, AQP4, SLC30A7, SLC40A1, SLC7A11 and SP1. The Hartung–Knapp–Sidik–Jonkman adjustment (27), which widens intervals when k is small and heterogeneity high, left one gene (ABCC4; FDR 0.013). With seven cohorts and median I^2 near 57%, the primary result describes the average of these cohorts rather than a prediction for a new one.

Table 3
Sensitivity analyses.

Analysis	Analysable	FDR < 0.05	High-confidence	Primary HC retained	Robust core retained
Primary	449	33	28	28/28	8/8
GSE153960 cervical cord only	449	36	27	26/28	8/8
GSE153960 lumbar cord only	449	31	27	24/28	8/8
Mean of probes per gene (all arrays)	449	53	36	28/28	8/8
Exon arrays: best (smallest-P) probeset	457	44	37	23/28	8/8
+ neuronal score (bulk cohorts)	449	47	38	28/28	8/8
+ neuronal + myeloid scores	449	19	14	12/28	8/8
+ neuronal + myeloid + astrocytic scores	449	17	11	9/28	8/8
Without the ten freeze-added genes	439	33	28	28/28	8/8

Each row changes one choice relative to the primary analysis. Composition scores are z-score means of marker transcripts (neuronal: SNAP25, SYT1, RBFOX3, NEFL, NEFM, STMN2, GAP43; myeloid: CD68,

AIF1, CSF1R, CD163, C1QB, TYROBP; astrocytic: GFAP, SLC1A2, GJA1, SOX9), entered as covariates in the two bulk cohorts; panel genes were excluded from marker sets. Leave-one-cohort-out results are in Table S6.

Leave-one-cohort-out analysis (Table S6) showed that GSE153960, the largest cohort, carries much of the result: without it, 18 genes were high-confidence and AQP4 and SLC40A1 fell just short of FDR < 0.05 (0.054 and 0.092) while keeping their direction in five of six cohorts. No other single cohort removed more than 8 of the 28.

Cell composition: two different questions

Bulk ALS spinal cord differs from control cord in its cells. In GSE153960 the myeloid marker score was 1.0 standard deviation higher in ALS and the astrocytic score 0.6 higher; a pan-neuronal score did not differ, as motor neurons are a small fraction of bulk cord. Adding the neuronal score alone did not reduce the result (38 high-confidence genes). Adding the myeloid score reduced it to 14 and adding the astrocytic score to 11; CP, FTL, NQO1, HMOX1, SOD2, IFI16, LRP1 and SLC39A14 were among the genes lost (Fig. 2; Table S5).

The unadjusted and adjusted analyses answer different questions. The unadjusted analysis asks whether the tissue's panel transcripts differ in ALS; for 28 genes they do. The adjusted analysis asks whether they differ beyond what the change in cell mix explains; for most genes they do not. Gliosis and microglial activation are part of ALS pathology, and they may be part of how detoxification biology changes in the disease, so adjustment can remove real biology as well as confounding. Both results are therefore reported, and neither is treated as the conservative version of the other. The eight core genes are those for which the answer to both questions is yes under every adjustment; nine of the 28 remain high-confidence in the fully adjusted model (Table 3).

Compartment

A separate pool of the five LCM cohorts and of the two bulk cohorts (defined after the results were seen; Table S4) placed 17 of the 28 genes in both compartments, 9 mainly in the LCM cohorts (including AQP4, SLC40A1, LRP1, NQO1 and ATP1B2) and 2 mainly in bulk cord (BACH1, CYP1B1). Several of the LCM-concentrated genes are predominantly astrocytic or vascular. Laser capture enriches motor neurons but does not purify them, and adherent astrocytic and endothelial processes carry over into captured material. These data therefore do not show that the signals are intrinsic to motor neurons.

How much does a conservative threshold hide?

Per-gene thresholds can miss a broad, low-amplitude shift across many genes. To measure how much signal a strict threshold hides, and whether a permissive threshold adds signal specific to the panel, the primary pipeline was run on all 27,028 genes measured in at least two cohorts. Panel genes were then

compared with random non-panel gene sets matched for the number of cohorts in which each gene is measured (Table 4). Matching matters: 96% of panel genes are measured in at least three cohorts against 73% of other genes, so any criterion that requires k ≥ 3 favours panel genes by coverage alone.

At the conservative end, panel genes were not over-represented: 35 were FDR-significant against a matched expectation of 41.5, and 29 were high-confidence against 26. At the permissive end — nominal P < 0.10 with the same direction in at least 70% of cohorts — the panel carried 113 genes against 101 expected, an excess of about 12 (P = 0.07). After composition adjustment that excess fell to about 6 (P = 0.27). The conservative threshold therefore hides little panel-specific signal: at most about a dozen consistently shifted genes, and those travel with the glial and myeloid response. These tiers and the permissive thresholds were defined after the primary result was seen and are exploratory. The companion methods manuscript reaches the same conclusion by competitive permutation across diseases (1).

Table 4
Graded evidence, with panel genes compared against coverage-matched random gene sets.

Evidence tier	Criterion	Panel genes (of 433, k ≥ 3)	Matched null, median [95% range]	Excess	P (≥ observed)	After myeloid adjustment: panel v null (P)
Conservative	BH-FDR < 0.05 (transcriptome-wide)	35	41.5 [31–54]	−6.5	0.91	20 v 29 (0.98)
Primary rule	High-confidence rule	29	26 [17–37]	+ 3	0.29	16 v 17 (0.64)
Exploratory	P < 0.05 and concordance ≥ 70%	89	78 [62–92]	+ 11	0.074	69 v 71 (0.63)
Exploratory	P < 0.10 and concordance ≥ 70%	113	101 [84–117]	+ 12	0.072	101 v 95 (0.27)
Exploratory	Concordance ≥ 70%, any P	213	202 [184–221]	+ 11	0.13	208 v 201 (0.23)

All criteria computed with the primary pipeline applied to 27,028 genes; FDR here is across all genes, so panel counts differ slightly from Table 2. Null: 1,000 random draws of non-panel genes with the same distribution of k (cohorts measured) as the 433 panel genes with k ≥ 3. The exploratory thresholds were chosen after the primary result was seen.

Graded reporting follows from this. The robust core (8 genes) is the claim least sensitive to analytic choices. The primary result (33 FDR-significant, 28 high-confidence) is the locked rule applied to correctly specified inputs. The exploratory layer — the 113 genes consistent in direction at P < 0.10, listed

in Data S1 — is offered for hypothesis generation only; the background test shows that it is only modestly enriched beyond what comparable genes would give.

Relation to the earlier locked analysis

An earlier analysis of the same seven cohorts, locked on 6 July 2026, reported 456 analysable genes, 26 FDR-significant and 22 high-confidence. Its GSE153960 input was a GEO2R comparison of all 1,011 ALS with all 288 control samples across every tissue; its GSE18920 input pooled motor-neuron and anterior-horn samples; its GSE26927 input counted replicate arrays as separate subjects; and its exon-array inputs used smallest-P probesets. The GPL5188 inputs of that analysis cannot be reproduced exactly from public files. The closest reconstruction (GSE56500 C9ORF72 cases only; GSE18920 motor-neuron samples only; smallest-P probesets) gives 28 FDR-significant and 23 high-confidence genes and retains 21 of the 22 earlier high-confidence genes (Table S1). Of the 22 earlier high-confidence genes, 14 remain high-confidence in the primary analysis here. SP3, SLC30A5, NFE2L2, PPARG, HPGDS, CYP4F3, UGT3A2 and SLC11A2 do not, although all keep their direction. The earlier text also cited per-dataset values from Student's t-tests with panel-restricted correction; those values are replaced here by the per-cohort estimates that entered the meta-analysis (Data S1).

Supporting anatomical screen within GSE153960

GSE153960 was also analysed region by region, with one value per donor and platform modelled (Table 5). The motor-cortex row combines medial, lateral and unspecified motor-cortex samples within donor. Effect-size-filtered panel hit rates (panel-restricted FDR < 0.05 and $|\log_2 FC| \geq 0.5$) were 24.6% in lumbar and 20.4% in cervical cord, 20.2% in cerebellum, 12–13% in motor and frontal cortex, 4% in thoracic cord and temporal cortex, and 0% in occipital cortex. Hippocampus (30 v 11 donors) was highest at 40.4%. Two features limit the interpretation. First, each regional panel rate was close to the transcriptome-wide rate in the same region (for example 20.4% v 17.7% in cervical cord), so the gradient describes how much each region changes overall rather than something specific to the panel. Second, occipital cortex showed no differential expression at any gene (0% transcriptome-wide), so its zero reflects a region with no detectable ALS change at 49 v 12 donors, not a panel-specific negative control. The screen is descriptive and is not the inferential result.

Table 5
Supporting region-stratified screen within GSE153960 (descriptive; not the inferential result).

Region	ALS / control donors	Panel genes measured	Panel FDR < 0.05	Panel FDR < 0.05 and $\|\log_2 FC\| \geq 0.5$	Up / down	Transcriptome-wide FDR < 0.05 and $\|\log_2 FC\| \geq 0.5$	Largest panel changes
Spinal cord, lumbar	147 / 44	398	69.3%	98 (24.6%)	72 / 26	18.9%	FMO1 + 1.58, SLC47A1 + 1.55, SLC22A2 + 1.53, ADH1B + 1.52; VWF − 1.12, CLDN5 -1.01, SLCO4A1 -0.96, CYP2A6 -0.88
Spinal cord, cervical	160 / 41	398	65.3%	81 (20.4%)	56 / 25	17.7%	AQP4 + 1.34, APOE + 1.29, SULT1C2 + 1.28, ABCA1 + 1.14; SELE − 1.49, VWF − 1.24, SLCO4A1 -1.07, CYP8B1 -1.02

Region	ALS / control donors	Panel genes measured	Panel FDR < 0.05	Panel FDR < 0.05 and $\lvert\log_2 FC\rvert \geq 0.5$	Up / down	Transcriptome-wide FDR < 0.05 and $\lvert\log_2 FC\rvert \geq 0.5$	Largest panel changes
Cerebellum	160 / 38	372	68.5%	75 (20.2%)	35 / 40	16.9%	CYP7A1 + 1.44, AQP4 + 1.26, CYP4F3 + 1.06, CYP2C19 + 0.95; SELE − 1.38, CYP2W1 -1.12, CLDN5 -1.12, VWF − 1.10
Motor cortex	143 / 32	404	55.0%	49 (12.1%)	16 / 33	11.1%	GSTA1 + 1.13, HPGDS + 0.72, CYP4F3 + 0.72, AQP1 + 0.69; SELE − 1.95, CYP2W1 -1.50, SOD3 -1.04, NQO1 -0.98
Frontal cortex	156 / 56	392	61.5%	50 (12.8%)	23 / 27	12.2%	CLDN11 + 0.84, GPX8 + 0.79, UGT8 + 0.71, ACSL4 + 0.64; SLC30A2 -1.00, CYP2W1 -0.99, SLC22A7 -0.77, ABCC3 -0.72

Region	ALS / control donors	Panel genes measured	Panel FDR < 0.05	Panel FDR < 0.05 and $\lvert\log_2 FC\rvert \geq 0.5$	Up / down	Transcriptome-wide FDR < 0.05 and $\lvert\log_2 FC\rvert \geq 0.5$	Largest panel changes
Occipital cortex	49 / 12	387	0.0%	0 (0.0%)	0 / 0	0.0%	—
Spinal cord, thoracic	47 / 11	398	6.0%	16 (4.0%)	14 / 2	2.9%	SULT1C2 + 1.16, ABCA1 + 1.12, AQP4 + 0.95, MAOB + 0.88; SELE − 2.95, TF -0.81
Temporal cortex	28 / 26	387	22.7%	17 (4.4%)	4 / 13	5.6%	SELE + 0.73, CYP4F3 + 0.67, ACSL4 + 0.65, CYP51A1 + 0.53; ANPEP − 0.92, CES1 -0.90, FMO3 -0.74, NOTCH3 -0.72
Hippocampus	30 / 11	396	59.8%	160 (40.4%)	105 / 55	38.4%	COX7C + 1.66, GLRX + 1.64, GLRX2 + 1.64, TXN + 1.62; SLC30A2 -1.45, CYP2D6 -1.17, SLC22A7 -1.15, CYP27B1 -1.09

PyDESeq2, one value per donor, design ~platform + group (hippocampus: one platform). Panel FDR is Benjamini–Hochberg across measured panel genes; the transcriptome-wide column applies the same

thresholds to all genes in that region for comparison. Motor cortex combines medial, lateral and unspecified samples within donor. Occipital cortex showed no differential expression at any gene.

Supporting per-cohort observations

Per-cohort estimates for every panel gene are in Data S1; within-cohort FDR below is across all genes measured in that cohort. In GSE18920 motor neurons, AQP4 was the strongest panel signal (+ 1.67, FDR 0.002), with SLC7A11 (+ 1.37), NQO1 (+ 0.87) and CP (+ 1.86) nominally higher (FDR 0.05–0.07). In GSE56500, CP (+ 1.09, FDR 0.03) and PECAM1 (+ 1.21, FDR 0.03) were higher. In GSE76220, 49 panel genes reached within-cohort FDR < 0.05, led by GSTM4, GSTM1, FTL, PECAM1, FMO2 and AQP1. GSE68605 had one panel gene at FDR < 0.05 (APOE, + 3.25). GSE19332 (3 v 7) and GSE26927 had none. In GSE19332 the direction of SQSTM1 depended on the probe (242568_s_at + 2.83, P = 0.012; 201471_s_at − 1.16, P = 0.042), so no claim about SQSTM1 is made.

Reproducibility between the two bulk cervical-cord cohorts was weak. Of 235 panel genes FDR-significant in GSE153960 cervical cord and measured in GSE26927, 45.5% had the same direction in GSE26927, and 46.6% of the 73 with $|\log_2 FC| \geq 0.5$ — no better than chance. GSE26927 is small (9 v 7 donors) and differs in platform and normalisation, and its per-gene estimates carry little weight in the meta-analysis. Two LCM cohorts also carry sizeable global offsets across all genes (median $\log_2 FC$ + 0.33 in GSE19332 and − 0.21 in GSE68605; Table S2), so part of their per-gene fold-changes reflects whole-array differences between groups.

Supporting model data: SOD1-G93A time-course (GSE10953)

The SOD1-G93A laser-capture time-course (28) samples motor neurons at defined disease stages, but has three animals per group, uncorrected P values and models familial SOD1 disease; it is supporting and hypothesis-generating only and does not enter the meta-analysis. Gpx4 was lower at all three timepoints: −0.702 (P = 0.016) at 60 days, − 0.683 (P = 0.037) at 90 days and − 0.974 (P = 0.021) at 120 days (Table S8). Fth1 was higher at 60 days (+ 1.244, P = 0.011). GPX4 reduces phospholipid hydroperoxides and its loss defines the committed step of ferroptosis (29,30); a lower transcript is not a demonstration of that step, and protein, enzyme activity and lipid peroxidation were not measured. GPX4 was not high-confidence in the human meta-analysis.

External context and independent direction checks

Published single-nucleus data provide cellular context that these bulk and LCM data cannot. Marker definitions from a human motor and prefrontal cortex atlas (31) place APOE, AQP4, AQP1 and SLC7A11 in a reactive-astrocyte module and CP and LRP1 in a vascular module. Per-subtype differential expression from a molecular-subtype study of the NYGC cohort (32) reports the astrocyte/iron module (APOE, AQP4, CP, FTL) upregulated in the ALS-Glia subtype in both cortex and spinal cord. A bulk transcriptomic study reports NFE2L2 and FOXO3 upregulated in frontal cortex and spinal cord (33).

These are published values on different units and are not pooled with the present estimates. Together with the composition analysis above, they indicate that much of the ALS panel signal has a glial or vascular source.

Two further cohorts that did not enter the meta-analysis were used, after the result was fixed, to check the direction of the 28 high-confidence genes, with complete GEO2R tables, the smallest-P probe per gene and a two-sided exact binomial test of sign agreement against 50%. In motor and frontal cortex RNA-seq from the NYGC cohort (GSE124439; 34), all 28 were measured and 19 changed in the same direction as the pooled estimate (68%, P = 0.087; Pearson r = 0.29; gene-label permutation P = 0.14). In whole blood (GSE112676; 35), 26 were measured (FTL and SP1 are absent from the array table) and 20 agreed in direction (77%, P = 0.0094; r = 0.24; permutation P = 0.24). Neither cohort is spinal cord or motor-neuron material, the cortex result does not reach significance, and the blood result is a direction check in a different tissue, not a replication of tissue transcript change.

Discussion

Analysed at the level of the donor, seven ALS cohorts yield a set of higher panel transcripts, consistently shifted across these cohorts, in ALS spinal cord and motor-neuron-enriched material. The most stable part of it is small: ABCA1, APOE, AQP1, AQP4, SLC30A7, SLC40A1, SLC7A11 and SP1 hold under every sensitivity analysis of the primary design, including removal of the cell-composition shift that dominates bulk ALS cord, and six of them hold without the largest cohort. That set connects cholesterol efflux (ABCA1, APOE), water homeostasis (AQP1, AQP4), iron export (SLC40A1), zinc transport (SLC30A7) and cystine import for glutathione synthesis (SLC7A11). Whether it reflects protective adaptation, injury or composition within the captured material is not determined by transcript abundance.

The broader primary set (28 genes) and the composition analysis tell a consistent story. The ferroxidase and ferritin transcripts (CP, FTL), NRF2-associated transcripts (NQO1, HMOX1, SOD2) and IFI16 are robust to analytic choices but not to adjustment for myeloid and astrocytic markers. They are best read as part of the glial and myeloid response to motor-neuron disease rather than as independent changes in detoxification capacity. This does not make them uninteresting. It places them in the cells in which a mechanistic test would need to be done.

The background comparison sets the limit on what the panel shows. At conservative thresholds the panel changes at the rate expected for comparable genes. At permissive thresholds it adds about a dozen consistently shifted genes beyond chance, and that excess does not survive composition adjustment. The concern that conservative reporting hides the biology is therefore testable, and here the answer is that it hides little that is specific to the panel. The panel remains a useful organising list for the genes that do change, and the exploratory layer is given in full in Data S1 so that others can follow individual genes. What the data do not support is a claim that detoxification genes as a class are preferentially disturbed in ALS tissue.

The earlier locked analysis reported 22 high-confidence genes from inputs that pooled every tissue of GSE153960 and both compartments of GSE18920. Its broad pattern — water channels, APOE, ABCA1, iron export, SLC7A11 — survives correction; eight of its genes do not. The revision is reported in full (Table S1) because the earlier numbers entered other manuscripts of this series.

The SOD1-G93A data place a lower Gpx4 transcript before symptom onset in that model. That is a statement about transcript timing in a familial model, not about ferroptosis, and GPX4 was not high-confidence in the human meta-analysis. Testing a ferroptosis hypothesis requires GPX4 protein and activity, direct lipid-peroxidation measurement and ferrostatin-class rescue in the same preparation.

Several limitations apply. First, all human data are postmortem and cross-sectional; they cannot separate upstream from reactive change. Second, the bulk cohorts reflect cell composition, and the marker-score adjustment is approximate: pan-neuronal markers do not capture motor-neuron loss in bulk cord, and adjustment may remove real biology. Third, laser capture enriches but does not purify motor neurons. Fourth, with seven cohorts and high heterogeneity the Hartung–Knapp–Sidik–Jonkman adjustment leaves one gene, so the pooled estimates describe these cohorts rather than predict a new one. Fifth, three LCM cohorts (GSE19332, GSE68605, GSE56500) come from one brain bank, and whether they share donors has not been verified; if they do, they are not independent. Sixth, the GSE68605 values were deposited after puma normalisation, and their log base has not been independently confirmed. Seventh, the exon-array inputs of the earlier analysis could not be reproduced exactly. Eighth, the panel is one curated selection, and the background test shows that comparable genes outside it change as often.

What these data supply is a donor-resolved transcript map of ALS for a pre-specified gene set, graded by how much each finding depends on analytic choices. Protein and activity measurement, cell-type-resolved differential expression and perturbation in a model that reproduces the human disease would be needed to turn any part of it into a mechanism.

Materials and Methods

Panel. The 468-gene panel was frozen on 5 July 2026 (MASTER_panel_FINAL_v468; Zenodo (16)). It was assembled by rule-based enumeration of functional families, and gene membership was fixed before the analyses reported here. Chronology: ALS analyses on earlier panel versions (238, 389 and 458 genes) preceded the freeze. The freeze added ten genes to the 458-gene version (CUL3, RBX1, AIFM2, GCH1, TF, TFRC, GLO1, HAGH, MFSD2A, FXN), and the result without them is reported (Table 3). Tier names follow the panel file, except that the tier labelled "ASD-maternal module" in the file is called the placental/sex-steroid module here.

Cohorts and contrasts. Sample groups were taken from GEO series-matrix characteristics (Table 1; sample-to-group assignments for every cohort are in the reproduction package). All contrasts are ALS minus control. For GSE153960, the "ALS Spectrum MND" group was compared with "Non-Neurological Control"; samples labelled Other Neurological Disorders, Other MND, pre-fALS or Unknown, and "ALS

Spectrum MND, Other Neurological Disorders", were excluded. NCBI-generated raw counts (GRCh38.p13) were summed within donor across cervical, lumbar and thoracic cord and analysed with PyDESeq2 0.5.4 (36,37) (size factors by poscounts; genes with ≥ 10 counts in at least as many donors as the smaller group; design ~platform + group). Platform is fully confounded with library preparation (manual v automated KAPA). For the regional screen the same model was fitted per region, with one value per donor.

Arrays. Microarray contrasts used a Python implementation of the GEO2R limma procedure (38) (automatic $\log_2$ transformation, complete cases, empirical-Bayes moderation). It reproduces the GEO2R tables of GSE19332, GSE68605, GSE26927, GSE56500 and GSE18920 exactly ($\log_2$FC within 5×10^{-8}). For GSE26927, replicate arrays (A05149, C037, C039, 1746) were averaged within donor before fitting. For the exon arrays, core probesets were averaged within transcript cluster using the GPL5188 annotation, and the first gene symbol of the cluster's gene assignment was used. GSE76220 was analysed with DESeq2 settings equivalent to GEO2R on NCBI-generated counts.

Meta-analysis. For each cohort one entry per gene symbol was used (the smallest-P probe on GPL570 and GPL6255; the gene-level estimate elsewhere), with SE = lfcSE for DESeq2 and $|\log_2FC/t|$ for limma. Genes measured in at least two cohorts were pooled by DerSimonian–Laird random effects (26), with two-sided normal P values and Benjamini–Hochberg FDR across analysable panel genes (25). The locked high-confidence rule was applied unchanged: FDR < 0.05, k ≥ 3, direction concordance ≥ 70%, and nominal P < 0.05 in at least two cohorts. Sensitivity analyses are listed in Table 3 and Tables S4–S6. The coverage-matched background test used 1,000 random draws of non-panel genes matched on k.

Composition. Marker scores (listed under Table 3) were z-score means of log-normalised expression per donor and were entered as covariates in the two bulk cohorts.

Declarations

Declaration of generative AI. During the preparation of this work the author used Grok (xAI), Claude (Anthropic) and Perplexity to assist with literature synthesis, bioinformatic pipeline construction, editorial refinement and critical review of claims and citations. After using these tools the author reviewed and edited the content as needed and takes full responsibility for the content. No generative tool is an author.

Ethics and human subjects.

The analyses used only publicly available, de-identified gene-expression data from NCBI GEO, which carry the ethical oversight of their originating studies. No identifiable private information was accessed, and no human subjects were enrolled.

Competing interests.

The author is the sole inventor on a filed patent application relating to panel-based research scoring methods that use the locked 468-gene list reported here. The application did not determine gene membership, the high-confidence rule or the reported results. Academic reuse of the deposited panel and code does not require a license from the author. The author declares no other competing interests.

Data and materials availability.

All primary data are public in NCBI GEO under the accessions in Table 1 and GSE10953. The locked panel, excluded-symbol list, per-disease meta counts and pipeline are deposited at Zenodo (16). For ALS, the deposited counts (version 1.0) and per-gene table (version 1.1) are those of the earlier analysis locked on 6 July 2026 (456 analysable, 26 FDR-significant and 22 high-confidence genes; see ‘Relation to the earlier locked analysis’); the donor-resolved results reported here are in Data S1. Per-gene results for every analysis (Data S1) and a reproduction package (scripts, GEO2R tables and sample lists) accompany this paper.

Funding.

This research received no external funding. All work was conducted independently through Sirius Neuroscience, LLC.

Author contributions.

M.E.M. is the sole author and performed all aspects of this work.

Acknowledgments.

The author thanks the New York Genome Center ALS Consortium and the Target ALS Human Postmortem Tissue Core, and the investigators who generated and deposited the GEO datasets analysed here, and acknowledges the participants in the original studies.

References

1. M. E. McCaulley, Transcriptomic associations of a pre-specified 468-gene redox and xenobiotic-metabolism panel across five neurological disorders, with a published-variant inventory. Methods-and-panel manuscript of this series, under peer review at Molecular Neurobiology (2026).
2. M. E. McCaulley, A locked 468-gene detoxification panel in Alzheimer’s disease brain, liver, and blood: 141 high-confidence cerebral associations including lower CYP46A1 transcript abundance, and a 12-sample hepatic CYP7A1 signal. Research Square, version 1 (2026). https://doi.org/10.21203/rs.3.rs-10999456/v1

3. M. E. McCaulley, Panel-gene transcriptomic associations and published-variant architecture in Parkinson disease. Research Square, version 1 (2026). https://doi.org/10.21203/rs.3.rs-11097203/v1
4. M. E. McCaulley, Panel-gene transcriptomic associations in multiple sclerosis: a three-cohort white-matter analysis of a locked 468-gene detoxification panel. Companion manuscript (2026).
5. M. E. McCaulley, A null adult postmortem-brain test of a locked 468-gene panel in autism spectrum disorder, with published maternal-axis architecture as context. Companion manuscript (2026).
6. R. H. Brown, A. Al-Chalabi, Amyotrophic lateral sclerosis. N. Engl. J. Med. 377, 162–172 (2017). https://doi.org/10.1056/NEJMra1603471
7. O. Hardiman et al., Amyotrophic lateral sclerosis. Nat. Rev. Dis. Primers 3, 17071 (2017). https://doi.org/10.1038/nrdp.2017.71
8. A. Chio et al., Global epidemiology of amyotrophic lateral sclerosis: a systematic review. Neuroepidemiology 41, 118–130 (2013). https://doi.org/10.1159/000351153
9. A. E. Renton, A. Chio, B. J. Traynor, State of play in amyotrophic lateral sclerosis genetics. Nat. Neurosci. 17, 17–23 (2014). https://doi.org/10.1038/nn.3584
10. J. P. Taylor, R. H. Brown Jr., D. W. Cleveland, Decoding ALS: from genes to mechanism. Nature 539, 197–206 (2016). https://doi.org/10.1038/nature20413
11. D. R. Rosen et al., Mutations in Cu/Zn superoxide dismutase gene are associated with familial amyotrophic lateral sclerosis. Nature 362, 59–62 (1993). https://doi.org/10.1038/362059a0
12. D. W. Cleveland, J. D. Rothstein, From Charcot to Lou Gehrig: deciphering selective motor neuron death in ALS. Nat. Rev. Neurosci. 2, 806–819 (2001). https://doi.org/10.1038/35097565
13. E. A. Winkler et al., Blood-spinal cord barrier disruption contributes to early motor-neuron degeneration in ALS-model mice. Proc. Natl. Acad. Sci. U.S.A. 111, E1035–E1042 (2014). https://doi.org/10.1073/pnas.1401595111
14. S. Garbuzova-Davis et al., Impaired blood-brain/spinal cord barrier in ALS patients. Brain Res. 1469, 114–128 (2012). https://doi.org/10.1016/j.brainres.2012.05.056
15. J. S. Henkel et al., Decreased mRNA expression of tight junction proteins in lumbar spinal cords of patients with ALS. Neurology 72, 1614–1616 (2009). https://doi.org/10.1212/WNL.0b013e3181a41228
16. M. E. McCaulley, Locked 468-gene detoxification panel, excluded-symbol list, per-disease meta counts and analysis pipeline. Zenodo, version 1.0 (2026), https://doi.org/10.5281/zenodo.22178094; version 1.1 (2026), https://doi.org/10.5281/zenodo.22181129; all versions, https://doi.org/10.5281/zenodo.22178093.
17. M. Prudencio et al., Truncated stathmin-2 is a marker of TDP-43 pathology in frontotemporal dementia. J. Clin. Invest. 130, 6080–6092 (2020). https://doi.org/10.1172/JCI139741
18. J. Humphrey et al., Integrative transcriptomic analysis of the amyotrophic lateral sclerosis spinal cord implicates glial activation and suggests new risk genes. Nat. Neurosci. 26, 150–162 (2023).

https://doi.org/10.1038/s41593-022-01205-3

19. P. Durrenberger et al., Common mechanisms in neurodegeneration and neuroinflammation: a BrainNet Europe gene expression microarray study. J. Neural Transm. 122, 1055–1068 (2015). https://doi.org/10.1007/s00702-014-1293-0
20. F. Krach et al., Transcriptome-pathology correlation identifies interplay between TDP-43 and the expression of its kinase CK1E in sporadic ALS. Acta Neuropathol. 136, 405–423 (2018). https://doi.org/10.1007/s00401-018-1870-7 (source publication of GSE76220).
21. L. E. Cox et al., Mutations in CHMP2B in lower motor neuron predominant amyotrophic lateral sclerosis (ALS). PLoS One 5, e9872 (2010). https://doi.org/10.1371/journal.pone.0009872
22. J. Cooper-Knock et al., C9ORF72 GGGGCC expanded repeats produce splicing dysregulation which correlates with disease severity in amyotrophic lateral sclerosis. PLoS One 10, e0127376 (2015). https://doi.org/10.1371/journal.pone.0127376
23. J. R. Highley et al., Loss of nuclear TDP-43 in amyotrophic lateral sclerosis (ALS) causes altered expression of splicing machinery and widespread dysregulation of RNA splicing in motor neurones. Neuropathol. Appl. Neurobiol. 40, 670–685 (2014). https://doi.org/10.1111/nan.12148
24. S. J. Rabin et al., Sporadic ALS has compartment-specific aberrant exon splicing and altered cell–matrix adhesion biology. Hum. Mol. Genet. 19, 313–328 (2010). https://doi.org/10.1093/hmg/ddp498
25. Y. Benjamini, Y. Hochberg, Controlling the false discovery rate: a practical and powerful approach to multiple testing. J. R. Stat. Soc. B 57, 289–300 (1995). https://doi.org/10.1111/j.2517-6161.1995.tb02031.x
26. R. DerSimonian, N. Laird, Meta-analysis in clinical trials. Control. Clin. Trials 7, 177–188 (1986). https://doi.org/10.1016/0197-2456(86)90046-2
27. J. IntHout, J. P. A. Ioannidis, G. F. Borm, The Hartung-Knapp-Sidik-Jonkman method for random effects meta-analysis is straightforward and considerably outperforms the standard DerSimonian-Laird method. BMC Med. Res. Methodol. 14, 25 (2014). https://doi.org/10.1186/1471-2288-14-25
28. L. Ferraiuolo et al., Microarray analysis of the cellular pathways involved in the adaptation to and progression of motor neuron injury in the SOD1 G93A mouse model of familial ALS. J. Neurosci. 27, 9201–9219 (2007). https://doi.org/10.1523/JNEUROSCI.1470-07.2007
29. W. S. Yang et al., Regulation of ferroptotic cancer cell death by GPX4. Cell 156, 317–331 (2014). https://doi.org/10.1016/j.cell.2013.12.010
30. B. R. Stockwell et al., Ferroptosis: a regulated cell death nexus linking metabolism, redox biology, and disease. Cell 171, 273–285 (2017). https://doi.org/10.1016/j.cell.2017.09.021
31. S. S. Pineda et al., Single-cell dissection of the human motor and prefrontal cortices in ALS and FTLD. Cell 187, 1971–1989 (2024). Data: NCBI SRA PRJNA1073234; Synapse syn51105515. https://doi.org/10.1016/j.cell.2024.02.031
32. K. O'Neill, R. Shaw, I. Bolger, NYGC ALS Consortium, O. H. Tam, H. Phatnani, M. Gale Hammell, ALS molecular subtypes are a combination of cellular and pathological features learned by deep

multiomics classifiers. Cell Rep. 44, 115402 (2025). https://doi.org/10.1016/j.celrep.2025.115402

33. N. P. Sneha, S. A. P. Dharshini, Y. H. Taguchi, M. M. Gromiha, Tracing ALS degeneration: insights from spinal cord and cortex transcriptomes. Genes 15, 1431 (2024). https://doi.org/10.3390/genes15111431
34. O. H. Tam et al., Postmortem cortex samples identify distinct molecular subtypes of ALS: retrotransposon activation, oxidative stress, and activated glia. Cell Rep. 29, 1164–1177.e5 (2019). https://doi.org/10.1016/j.celrep.2019.09.066
35. W. van Rheenen et al., Whole blood transcriptome analysis in amyotrophic lateral sclerosis: a biomarker study. PLoS One 13, e0198874 (2018). https://doi.org/10.1371/journal.pone.0198874
36. B. Muzellec, M. Telenczuk, V. Cabeli, M. Andreux, PyDESeq2: a python package for bulk RNA-seq differential expression analysis. Bioinformatics 39, btad547 (2023). https://doi.org/10.1093/bioinformatics/btad547
37. M. I. Love, W. Huber, S. Anders, Moderated estimation of fold change and dispersion for RNA-seq data with DESeq2. Genome Biol. 15, 550 (2014). https://doi.org/10.1186/s13059-014-0550-8
38. M. E. Ritchie et al., limma powers differential expression analyses for RNA-sequencing and microarray studies. Nucleic Acids Res. 43, e47 (2015). https://doi.org/10.1093/nar/gkv007

Figures

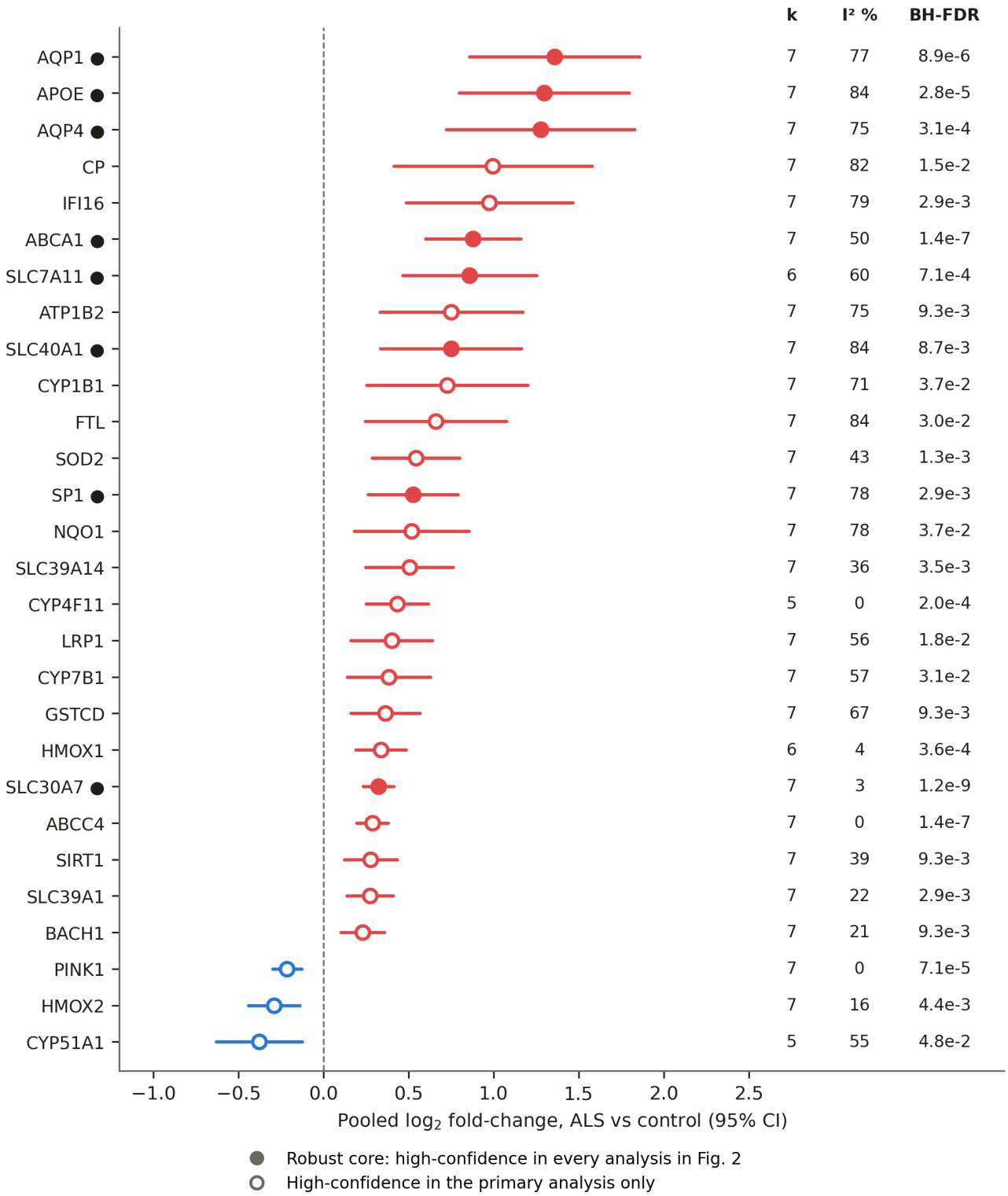


Figure 1

The 28 high-confidence genes of the primary seven-cohort random-effects meta-analysis. Points are pooled log2 fold-changes (ALS v control) with 95% confidence intervals; red = higher in ALS, blue = lower. Filled points and ● mark the eight-gene robust core (high-confidence in every analysis in Fig. 2). k, I² and BH-FDR are printed at right. The dashed line marks no change.

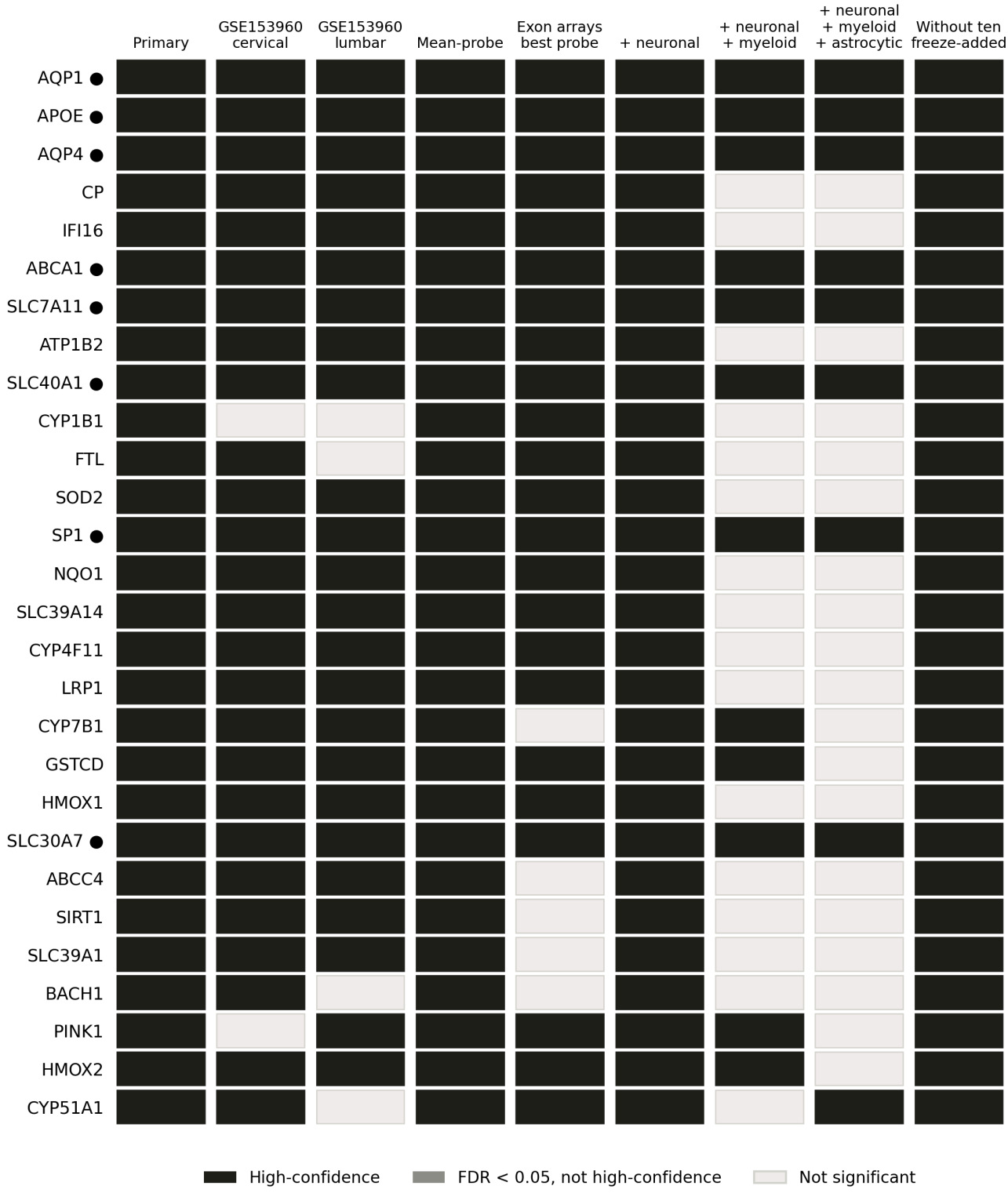


Figure 2

High-confidence status of the 28 primary genes across nine analyses. Dark = high-confidence; intermediate = FDR < 0.05 but not high-confidence; light = not FDR-significant. Rows marked ● are the robust core. Columns: primary analysis; GSE153960 restricted to cervical or lumbar cord; mean of probes on all arrays; exon arrays by smallest-P probeset; bulk cohorts adjusted for neuronal, neuronal + myeloid, and neuronal + myeloid + astrocytic marker scores; panel without the ten freeze-added genes.

Supplementary Files

This is a list of supplementary files associated with this preprint. Click to download.

- McCaulleyALS468panelSupplementaryMaterials20261014.docx
- McCaulleyALSDataS1metapergene20260929.xlsx
- McCaulleyALSreproductionpackage20260929.zip